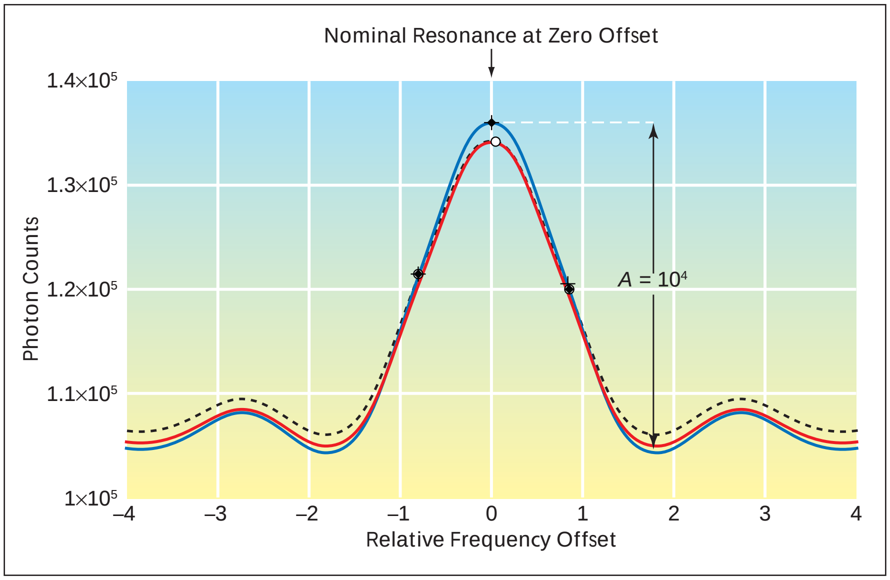

These Three Plots represent fits of the nonlinear curve to three sets of simulated measurements, each set comprising photon counts at relative frequency offsets (y values) of 0 and ±0.761. The parameters of the simulated measurements were B = 1.05 × 10^5 counts, A = 3 × 10^4 counts, and signal-to-noise ratio ≈30.

frequency, the oscillator signal is applied in a square pulse of the oscillator signal having a suitable duration (typically, of the order of a second), and, for each pulse at each frequency offset, fluorescence photons of the transition in question are counted. As described below, the counts are used to determine a new nominal resonance frequency. Thereafter, offsets are determined with respect to the new resonance frequency. The process as described thus far is repeated so as to repeatedly adjust the oscillator to track the most recent estimate of the nominal resonance frequency.

The theoretical nonlinear curve is that of the Rabi equation for the shape of the resonance peak

$$P(y) = \frac{\sin^2\left(\frac{\pi}{2}\sqrt{1+y^2}\right)}{1+y^2}$$

where the dimensionless variable y is related to the duration of the microwave pulse, T, and the frequency offset $\nu - \nu_0$ from the atomic absorption frequency, ν_0 , as follows: $y = 2T(\nu - \nu_0)$.

Assuming that the signal power has been optimized and that the photon count at a given measurement signal frequency includes a non-resonant background contribution plus a contribution attributable to the resonance, the basic measurement equation for the ith measurement is

$$C(i) = B + AP(y_1 - \varepsilon)$$

where $C(i)$ is the atomic fluorescence photon count, A is atomic fluorescence, and ε is an offset of the nominal resonance frequency from the actual resonance frequency. If measurements are made at three different oscillator frequency offsets (y_1, y_2, y_3), then one has

$$C(1) = B + AP(y_1 - \varepsilon)$$
$$C(2) = B + AP(y_2 - \varepsilon)$$
$$C(3) = B + AP(y_3 - \varepsilon)$$

Repeatedly, for the most recent such set of three measurements (see figure), this set of three equations is inverted to extract B, A, and ε from the measurement values $C(1)$, $C(2)$, and $C(3)$. Because the solution obtained through inversion of the three equations separates the influences of background light, signal strength, and the offset of the resonance from the nominal resonance frequency, unlike in a prior method, drift in the power of the lamp used to excite the clock atoms to the upper level of the transition does not seem to effect frequency pulling (that is, it does not seem to force a change in the estimate of the resonance frequency).

This work was done by John D. Prestage, Sang K. Chung, and Meirong Tu of Caltech for NASA's Jet Propulsion Laboratory. Further information is contained in a TSP (see page 1). NPO-45958

Measurement of the Length of an Optical Trap

This technique aids in the assembly of MEMS devices.

John H. Glenn Research Center, Cleveland, Ohio

NASA Glenn has been involved in developing optical trapping and optical micromanipulation techniques in order to develop a tool that can be used to probe, characterize, and assemble nano and microscale materials to create microscale sensors for harsh flight environments. In order to be able to assemble a sensor or probe candidate sensor material, it is useful to know how far an optical trap can "reach"; that is, the distance beyond / below the stable trapping point through which an object will be drawn into the optical trap. Typically, to measure the distance over which an optical trap would influence matter in a horizontal (perpendicular to beam propagation) direction, it was common to hold an object in one optical trap, place a second optical trap a known distance away, turn off the first optical trap, and note if the object was moved into the second trap when it was turned on. The disadvantage of this technique is that it only gives information of trap influence distance in horizontal (x–y) directions. No information about the distance of the influence of the trap is gained in the direction of propagation of the beam (the z direction).

A method was developed to use a time-of-flight technique to determine the length along the propagation direction of an optical trap beam over which an object may be drawn into the optical trap. Test objects (polystyrene microspheres) were held in an optical trap in a water-filled sample chamber and raised to a pre-determined position near the top of the sample chamber. Next, the test objects were released by blocking the optical trap beam. The test objects were allowed to fall through the water for predetermined periods of time, at the end of which the trapping beam was unblocked. It was noted whether or not the test object returned to the optical trap or continued to fall.

This determination of the length of an optical trap's influence by this manner assumes that the test object falls through the water in the sample chamber at terminal velocity for the duration of its fall, so that the distance of trap influence can be computed simply by: $d = V_T t$, where d is the trap length (or distance of trap reach), V_T is the terminal velocity of the test object, and t is the time interval over which the object is allowed to fall. In order for this methodology to work, it must be established that the test object indeed falls through the water in the sample chamber at terminal velocity. This answers the question of how far below the trap point an object must be to be drawn into an optical trap in order to select and manipulate material for microscale assembly and characterization.

This methodology would make it possible for optical trapping to be incorporated into the assembly of MEMS (microelectromechanical systems) devices. In particular, adding pieces or connectors to MEMS devices that cannot be positioned via photolithography and vapor or film deposition techniques may be added to a MEMS device via placement by optical traps. In this case, it is imperative to know how far beyond the stable trapping point in the direction of propagation of the beam an object should or must be to be trapped, and also the distance beyond the stable optical trapping point over which the propagating laser beam has no effect.

This work was done by Susan Y. Wrbanek of Glenn Research Center. Further information is contained in a TSP (see page 1).

Inquiries concerning rights for the commercial use of this invention should be addressed to NASA Glenn Research Center, Innovative Partnerships Office, Attn: Steve Fedor, Mail Stop 4–8, 21000 Brookpark Road, Cleveland, Ohio 44135. Refer to LEW-18539-1.

Phase-Array Approach to Optical Whispering Gallery Modulators

NASA's Jet Propulsion Laboratory, Pasadena, California

This technology leverages the well-defined orbital number of a whispering gallery modulator (WGM) to expand the range of applications for such resonators. This property rigidly connects the phase variation of the field in this mode with the azimuthal angle between the coupling locations.

A WGM with orbital momentum L has exactly L instant nodes around the circumference of the WGM resonator supporting such a mode. Therefore, in two locations separated by the arc α, the phase difference of such a field will be equal to $\phi = \alpha L$. Coupling the field out of such locations, and into a balanced interferometer, once can observe a complete constructive or distractive interference (or have any situation in between) depending on the angle α. Similarly, a mode $L + \Delta L$ will pick up the phase $\phi + \alpha\Delta L$.

In all applications of a WGM resonator as a modulator, the orbital numbers for the carrier and sidebands are different, and their differences ΔL are known (usually, but not necessarily, $\Delta L = 1$). Therefore, the choice of the angle α, and of the interferometer arms difference, allows one to control the relative phase between different modes and to perform the conversion, separation, and filtering tasks necessary.

This work was done by Dmitry Strekalov of Caltech for NASA's Jet Propulsion Laboratory. Further information is contained in a TSP (see page 1).

This invention is owned by NASA, and a patent application has been filed. Inquiries concerning nonexclusive or exclusive license for its commercial development should be addressed to the Patent Counsel, NASA Management Office–JPL. Refer to NPO-45730.

Infrared Camera System for Visualization of IR-Absorbing Gas Leaks

This system is applicable in HVAC, methane production plants, and oil refineries.

John F. Kennedy Space Center, Florida

Leak detection and location remain a common problem in NASA and industry, where gas leaks can create hazardous conditions if not quickly detected and corrected. In order to help rectify this problem, this design equips an infrared (IR) camera with the means to make gas leaks of IR-absorbing gases more visible for leak detection and location.

By comparing the output of two IR cameras (or two pictures from the same camera under essentially identical conditions and very closely spaced in time) on a pixel-by-pixel basis, one can cancel out all but the desired variations that correspond to the IR absorption of the gas of interest. This can be simply done by absorbing the IR lines that correspond to the gas of interest from the radiation received by one of the cameras by the intervention of a filter that removes the particular wavelength of interest from the "reference" picture. This can be done most sensitively with a gas filter (filled with the gas of interest) placed in front of the IR detector array, or (less sensitively) by use of a suitable line filter in the same location.

This arrangement would then be balanced against the unfiltered "measurement" picture, which will have variations from IR absorption from the gas of interest. By suitable processing of the signals from each pixel in the two IR pictures, the user can display only the differences in the signals. Either a difference or a ratio output of the two signals is feasible. From a gas concentration viewpoint, the ratio could be processed to show the column depth of the gas leak. If a variation in the background IR light intensity is present in the field of view, then large changes in the difference signal will occur for the same gas column concentration between the background and the camera. By ratioing the outputs, the